

Barramundi (*Lates calcarifer*) rare coloration patterns: a multiomics approach to understand the “panda” phenotype

Roberta Marcoli¹  | David B. Jones¹ | Cecile Massault¹ | Paul J. Harrison^{1,2} | Holly S. Cate^{1,2} | Dean R. Jerry^{1,3}

¹ARC Research Hub for Supercharging Tropical Aquaculture through Genetic Solutions, James Cook University, Townsville, Queensland, Australia

²Mainstream Aquaculture Group Pty Ltd, Werribee, Victoria, Australia

³Tropical Futures Institute, James Cook University, Singapore, Singapore

Correspondence

Roberta Marcoli, ARC Research Hub for Supercharging Tropical Aquaculture through Genetic Solutions, James Cook University, Queensland, Australia.

Email: roberta.marcoli@jcu.edu.au

Abstract

The barramundi (*Lates calcarifer*), a significant aquaculture species, typically displays silver to bronze coloration. However, attention is now drawn to rare variants like the “panda” phenotype, characterized by blotch-like patterns of black (PB) and golden (PG) patches. This phenotype presents an opportunity to explore the molecular mechanisms underlying color variations in teleosts. Unlike stable color patterns in many fish, the “panda” variant demonstrates phenotypic plasticity, responding dynamically to unknown cues. We propose a complex interplay of genetic factors and epigenetic modifications, focusing on DNA methylation. Through a multiomics approach, we analyze transcriptomic and methylation patterns between PB and PG patches. Our study reveals differential gene expression related to melanosome trafficking and chromatophore differentiation. Although the specific gene responsible for the PB–PG difference remains elusive, candidate genes like *asip1*, *asip2*, *mlph*, and *mreg* have been identified. Methylation emerges as a potential contributor to the “panda” phenotype, with changes in gene promoters like *hand2* and *dynamain* possibly influencing coloration. This research lays the groundwork for further exploration into rare barramundi color patterns, enhancing our understanding of color diversity in teleosts. Additionally, it underscores the “panda” phenotype's potential as a model for studying adult skin coloration.

KEYWORDS

Asian seabass, melanophore, multiomics, pigmentation, teleosts

1 | INTRODUCTION

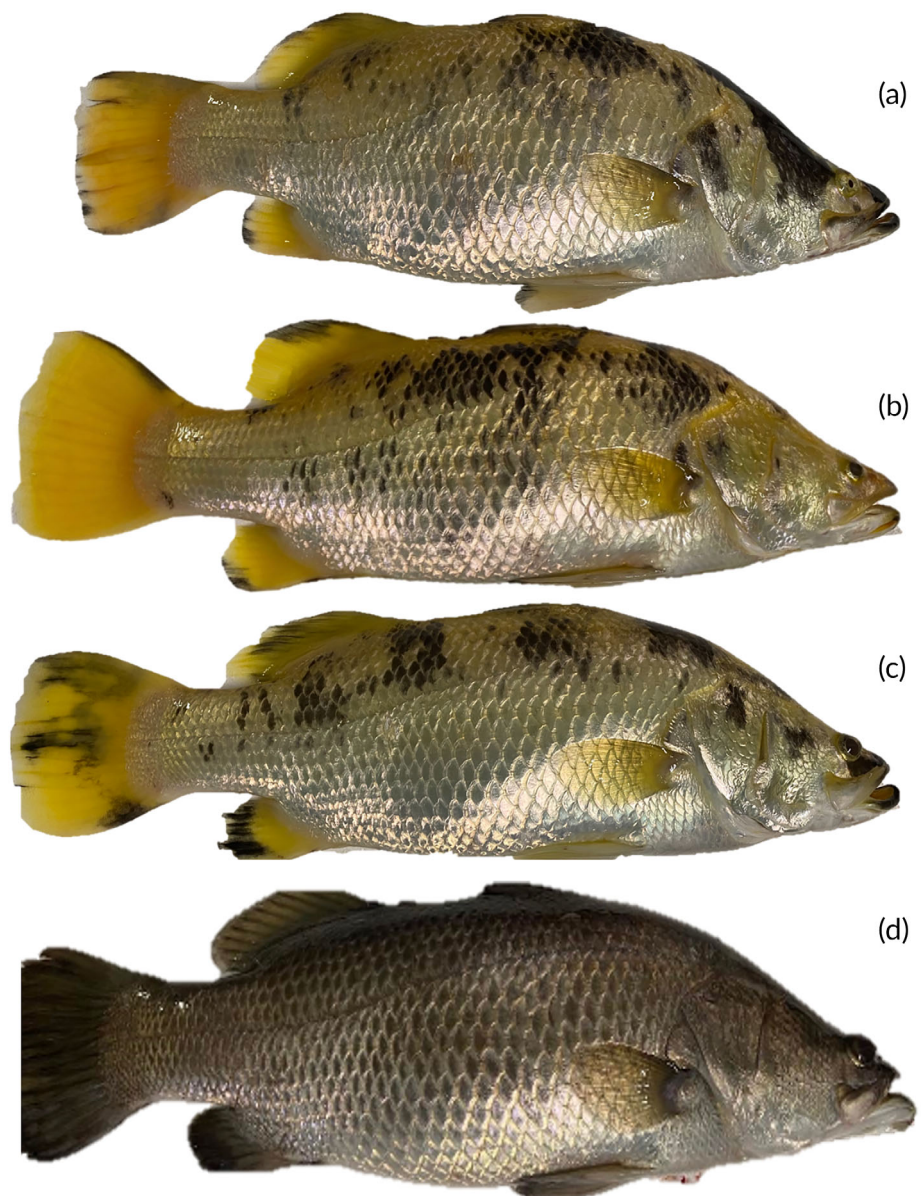
Barramundi (*Lates calcarifer*), also known as Asian seabass, is a species native to tropical regions of the Indo-Pacific and is of importance in aquaculture, capture, and recreational fisheries (Jerry, 2013). The typical skin coloration of barramundi varies from silver to bronze, but this species also exhibits several rare skin color variants, including the “golden”, “platinum”, “black” and “panda” phenotypes (Marcoli et al., 2023). The

“panda” phenotype, as its name implies, is characterized by a blotch-like pattern, with a combination of silver, black (PB), and golden (PG) skin patches (Figure 1). Prior histological and cytological research, which examined the skin coloration among barramundi color morphs, highlighted differences in the composition of skin cell populations between different color phenotypes in barramundi (Marcoli et al., 2023). This study specifically examined the differences between the two-color patches of barramundi in the “panda” phenotype, analyzing fin tissues at

This is an open access article under the terms of the [Creative Commons Attribution](https://creativecommons.org/licenses/by/4.0/) License, which permits use, distribution and reproduction in any medium, provided the original work is properly cited.

© 2024 The Author(s). *Journal of Fish Biology* published by John Wiley & Sons Ltd on behalf of Fisheries Society of the British Isles.

FIGURE 1 Barramundi (*Lates calcarifer*) color variants examined in this study: (a, b, c) “panda” phenotype, (d) wild type. (a) Sample P1, (b) sample P2, (c) sample P3, and (d) wild-type barramundi (for this present study no samples were taken from the wildtype phenotype).



the boundary between PB and PG using various techniques such as histological, immunohistochemical, and ultrastructural analysis (Marcoli et al., 2023). In accordance with the different techniques used, the study demonstrated that differences in the presence and abundance of melanin-producing (stages 2, 3, and 4) melanophores were the major driver of the difference in coloration between PG and PB (Marcoli et al., 2023). Furthermore, an analysis of the transcriptome profile distinguishing the golden phenotype from the wildtype silver phenotype showed that multiple genes related to the melanin production were altered between the two color variants (Marcoli et al., 2024); the underlying molecular basis influencing the black and gold patches in “panda” barramundi within the same individual, however, has not been examined. The unique pigmentation exhibited by “panda” barramundi not only enhances the appeal of this species in the aquarium and commercial aquaculture trades, but also could serve as a potential model for studying the molecular mechanisms governing color changes in teleosts.

While many studies have investigated color pattern formation in teleosts (Irion & Nüsslein-Volhard, 2019; Tian et al., 2022), most of the literature available is associated with investigating the basis of regular (and wild-type) stripe-like patterning (Gur et al., 2020; Johnson et al., 1995; Kondo et al., 2021; Singh & Nüsslein-Volhard, 2015; Yamaguchi et al., 2007) and changes in dorso-ventral pattern coloration (Ahi & Sefc, 2017; Cal et al., 2019), and to date there is only limited research conducted in fish relating to phenotypes representing a random blotch-like pattern coloration (Fang et al., 2022; Luo et al., 2018; Santos et al., 2016). These studies involve the melanic side-spotting patterns in *Poeciliid* guppies (Zerulla & Stoddard, 2021) and the multiple coloration patterns within individuals of koi carp (*Cyprinus rubrofasciatus*) (Dong et al., 2020; Luo et al., 2018; Tian et al., 2022). However, unlike patterning in most other teleosts, where the coloration is considered mainly static once developed (or within the life stage that characterized it) (Kratochwil &

Mallarino, 2023), the “panda” barramundi exhibits a remarkably plastic phenotype, showcasing changes in the positioning of the color patches in response to unknown cues (Data S1). This phenotypic plasticity suggests a complex interplay between genetic and epigenetic factors, prompting an exploration into the transcriptomic and methylation profiles associated with the “panda” variant.

DNA methylation is a significant epigenetic alteration found in DNA. It is essential for maintaining the biological functions of higher organisms (Moore et al., 2013) and is involved in various processes such as genomic imprinting, X chromosome inactivation, aging, and carcinogenesis (Mhanni & McGowan, 2002). DNA methylation at promoter sites frequently acts as a transcriptional repressor by suppressing gene expression, leading to a negative association between DNA methylation status and gene expression level (Robertson & Jones, 2000). Previous studies with teleosts have examined transcriptomic changes linked to pigmentation patterns, but very few have used a multiomics approach to analyze the relationship between methylation, changes in gene expression, and physical characteristics (Li et al., 2015; Liu et al., 2022; Zhang et al., 2017). It is noteworthy that no study has examined DNA methylation changes related to color patch variation within the same individual, but the relationship between coloration, gene expression, and microRNA-induced gene regulation has been proposed as the epigenetic and cellular mechanism underlying the species' individual color variations in koi carp (Dong et al., 2020; Luo et al., 2018; Tian et al., 2022). Given the complexity of epigenetic factors and how they modulate transcription, it is possible that multiple molecular mechanisms might interplay to influence dynamic color pattern formation in teleosts.

Through the analysis of the “panda” barramundi transcriptome and methylation patterns, the objective of this study was to establish a fundamental understanding of the molecular mechanisms underlying color changes and the color plasticity in the species, but also to utilize the “panda variant” as a valuable model for investigating coloration in fish. The findings of this study may have broader implications beyond the understanding of the rare “panda” phenotype in barramundi, offering an insightful comprehension into the color diversity and blotch-like pattern formation in teleosts more broadly.

2 | MATERIALS AND METHODS

2.1 | Experimental design and sampling

Three individual barramundi representing the “panda” color variant (mean weight 0.62 ± 0.09 kg, mean length 34.1 ± 1.1 cm) were obtained from a commercial population (Mainstream Aquaculture Group). The fish were housed in a 2000-L tank that was part of a 10-tank recirculating tank system. Three times per day, the fish were fed a commercial aquaculture feed to satiety. The animals were closely monitored during feeding and routinely inspected throughout the day. The photoperiod was set to correspond with daylight, with lights turned off at night. Sampled fish were sedated in 0.2 mL/L Aqu-i-S (Aqu-i-S New Zealand Ltd.) (JCU ethics approval: A2829) and approximately 1-cm² dorsal fin samples were taken.

Two separate samples were taken for each fish: a sample from the golden-colored patch (PG) and one from the black-colored patch (PB). The samples were placed in RNeasy Lysis Solution (Qiagen) and stored at -80°C prior to RNA and DNA extraction.

2.2 | DNA and RNA isolation and library preparation

DNA and RNA were isolated from the same fin tissue sampled to directly compare gene expression with methylation levels. The RNA extraction methodology is outlined in the study conducted by (Marcoli et al., 2024). The AllPrep DNA/RNA Kits (Qiagen) were used to isolate total DNA from approximately 100 mg of fin tissue for methylation analysis. The DNA that was obtained was subjected to RNase treatment to remove any residual RNA. The initial quality of DNA was assessed by evaluating absorbance ratios at optical density (OD) 260/280 and OD 260/230 using a NanoDrop® ND-1000 UV-Vis spectrophotometer. Furthermore, the evaluation of DNA quality was conducted through the utilization of 1.5% agarose gel electrophoresis. This involved visually examining the gel under ultraviolet light to verify the absence of any potential RNA contamination bands. The DNA samples were subsequently stored at a temperature of -80°C prior to their transfer to the Australian Genome Research Facility for subsequent quantification using an Agilent DNA Bioanalyzer chip (<https://www.agilent.com/>). Library preparation for Whole Genome Enzymatic Methylation Sequencing (WGEMS) was undertaken using a NEBNext Enzymatic Methyl-seq kit before pair-end sequencing on an Illumina NovaSeq S4 Lane, 300 cycles, yielding 150 bp reads.

2.3 | Transcriptome and methylome analysis

The transcriptome methodology was described in Marcoli et al. (2024). In brief: FeatureCounts (Galaxy Version 2.0.1 + galaxy2), MultiQC (Galaxy Version 1.11 + galaxy1) (Ewels et al., 2016), and the DESeq2 packages (Galaxy Version 2.11.40.7 + galaxy2) (Love et al., 2014) were utilized to compare the three golden patches (PG) to the three black patches (PB) of the “panda” barramundi. Differentially expressed genes (DEGs) selected for further analysis were chosen when $|\log_2\text{FC}| \geq 1$ (fold change [FC] >2 or <0.5) and with adjusted $p < 0.05$.

Following WGEMS sequencing, the FASTQ files were quality checked and the adapter trimmed using the Galaxy platform version 22.05. In brief, FastQC (Galaxy Version 0.73 + galaxy0) (Andrews, 2010), Trim Galore! (Galaxy Version 0.6.7 + galaxy0 - adapter: Illumina Universal Adapter) (Krueger et al., 2021), Bwameth (Galaxy Version 0.2.6 + galaxy0) (Pedersen et al., 2014), rmdup (Li et al., 2009), and methylDackel (<https://github.com/dpryan79/MethylDackel>) were utilized to generate the CpG coverage for further analysis (output option: MethylKit).

Utilizing the MethylKit software, the statistical method used to detect differentially methylated cytosines (DMCs) between groups was logistic regression, with thresholds of False Discovery Rate <0.01 and minimum difference in methylation of 25%. PB coloration of barramundi

was considered as reference. For each DMC site, if the PG compared to the PB had a methylation level at least of 25% higher, then that DMC was considered hypermethylated. Alternatively, if the methylation level was 25% lower in PG compared to the PB, then the DMC was considered hypomethylated. Tools such as Integrated Genome Viewer, Chip Seeker, ShinyGO (Version 0.76.3), String, and KOBAS (Version 3.0) were used for gene ontology enrichment analysis.

2.4 | Transcriptome-methylome association

To associate differential methylation with the transcriptome analysis, genes that were considered to be both differentially methylated genes (DMGs) and DEGs were selected and classified as differentially expressed-methylated genes (DEMG). DEMG gene reference ID was utilized for enrichment analysis with ShinyGO and KOBAS software. To further analyze the data, the DEMGs that had a DMC in the promoter or transcription start site were further analyzed, plotted, and classified as differentially expressed-methylated genes in the promoter (pDEMGs). Considering the knowledge that promoter methylation and gene expression are inversely proportional, only genes with hypermethylation-downregulation and hypomethylation-upregulation were selected and classified as inversely proportional differentially expressed-methylated genes in the promoter (ipDEMGp). To examine the effect of DNA methylation on the local regulation of gene expression, the Pearson correlation (R) between the percentage of methylation and the normalized expression values (Z-score) of the corresponding genes was calculated. Importantly, some gene promoters contained multiple CpGs and consequently the correlation coefficient was calculated for each CpG(promoter)-gene expression pair. $|R| > 0.5$ and p -adjusted < 0.05 were set as the significance threshold for correlations.

3 | RESULTS

3.1 | Overview of the RNA-seq data

Sequencing of the mRNA libraries of the two skin color patches resulted in >100 M reads per library (Data S2). In total 126.50 Gb of data yield was generated, with average raw reads of $100,652,663 \pm 3,639,011$ for the three PG fish and $113,572,913 \pm 2,318,750$ for the three PB fish. The average GC content was 48.4% and the read length 150 bp. The average numbers of clean reads between samples of the same variants were $100,530,463 \pm 3,646,274$ for PG and $113,441,479 \pm 2,310,682$ for PB. The reads were mapped to the *Lates calcarifer* genome (Vij et al., 2016) for analysis, and the average percentage of uniquely mapped genes among the samples was 83.46%.

3.2 | DEG analysis among PG and PB of “panda” barramundi

3.2.1 | Pairwise comparison and DEG analysis

Pairwise comparisons of DEGs were plotted to identify gene expression differences between PG and PB (Figure 2a). Analyses showed 1601 genes exhibiting differential expression between PG and PB; 930 genes, equivalent to 58.08%, were downregulated in PG, while 671, equivalent to 41.91%, were upregulated in PG. To reveal the differences underlying the molecular basis in the color pattern formation in “panda” barramundi the DEGs from the pairwise comparison between PG and PB were evaluated, and the Z-score for each gene was generated and plotted as a heatmap to visualize the gene expression difference for each DEG in each sample (Figure 2b), with the top Kyoto Encyclopedia of Genes and Genomes (KEGGs) and Gene Ontology (GOs) shown in Figure 3a. Pathways related to inflammation and

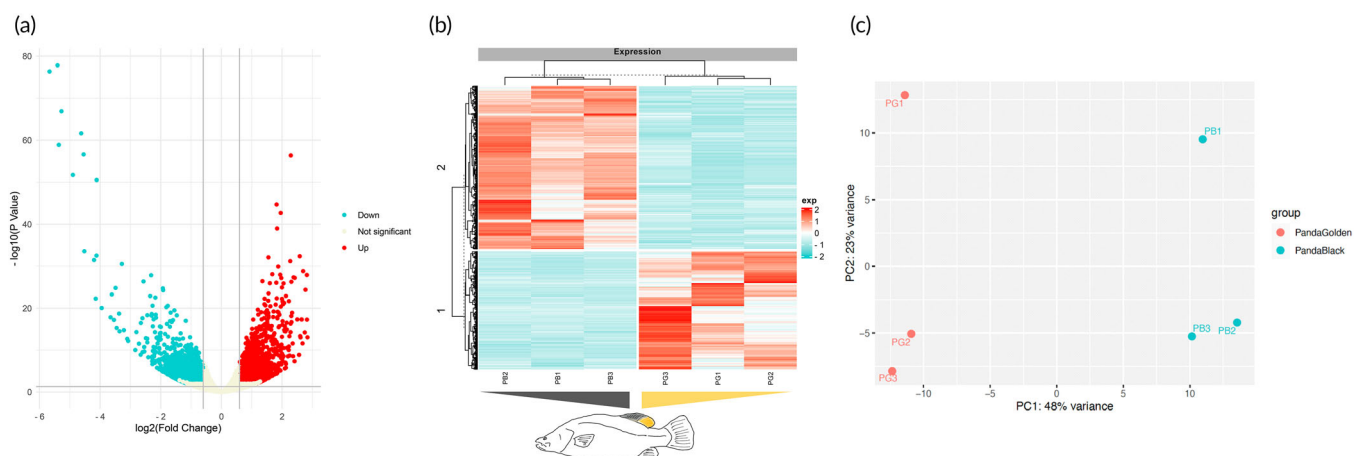


FIGURE 2 (a) Volcano plots of “panda-golden” (PG) vs. “panda-black” (PB) barramundi. (b) Heatmap representing Z-scores of differentially expressed genes (DEGs) between PG and PB. Light blue, downregulation; red, upregulation. (c) Principal coordinates analysis of gene expression patterns of color variants (group) of *Lates calcarifer*.

immune systems (neutrophil activation, granulocyte activation, inflammatory response, immune response) were found to be enriched within the biological process, while in the KEGGs pathways cell adhesion molecules, phagosome, tyrosine metabolism, and melanogenesis were among the pathways found to be enriched.

3.2.2 | Principal component analysis

Principal component analysis (PCA) among the two fin colors showed that 71% of the global variation in gene expression was explained by the first two principal components (PC1 48% and PC2 23%) (Figure 2c). Samples representing a similar color variant (PG or PB) clustered in the multidimensional space, indicating that each color variant generally had a distinct pattern of gene expression.

3.3 | Normalized counts of genes associated to the melanin pathway

3.3.1 | Melanin- and melanophore-associated genes

To delve deeper into the function of the pathways identified in the skin color variations of barramundi, we examined the normalized expression of genes associated with melanophores and melanogenesis pathways. *Adcyap1r1b* and *asip1* followed the same pattern of expression with PG showcasing a significant upregulation, compared to PB (Figure 3b). *asip2b*, *prkcab*, *dct*, *camk2b1*, *alx3*, *mreg*, and *mlph* followed the same pattern of expression, with PG showcasing a significant downregulation, in comparison to PB (Figure 3b).

3.4 | Overview of the whole-genome enzymatic sequencing data

To better understand barramundi methylome changes between PG and PB color patches, WGEMS libraries were sequenced and quality checked using Illumina sequencing technology. Each library yielded an average of 106,923,106 sequence reads. For analysis, the reads were mapped to the *Lates calcarifer* genome, with an average percentage of uniquely mapped reads to the bisulphite converted genome of 99.7%. Individual samples and compared groups (PG vs. PB) did not differ significantly in terms of raw, trimmed, or mapped reads. The per-base methylation metrics were extracted from the mapped reads for further analysis. Routine checks were performed within the MethyKit package (Akalin et al., 2012) to assess the quality of the CpG extracted sites, where the histogram of % of CpG methylation for each sample (Data S3) represents a normal distribution; additionally, the absence of a peak on the right side of the histogram (Data S4) indicates that the data did not contain polymerase chain reaction (PCR) duplicates.

3.4.1 | Differentially methylated cytosine analysis among color variants: PCA and sample clustering

A total of 160,460 CpG positions that were found in every sample at least once were used for analysis of differential methylation between color morphs, and of those 4877 were differentially methylated between the two groups. PCA among PG and PB fin colors, based on DMCs, showed that 92.83% of the global variation in methylation was explained by the first two principal components (PC1 63.8% and PC2

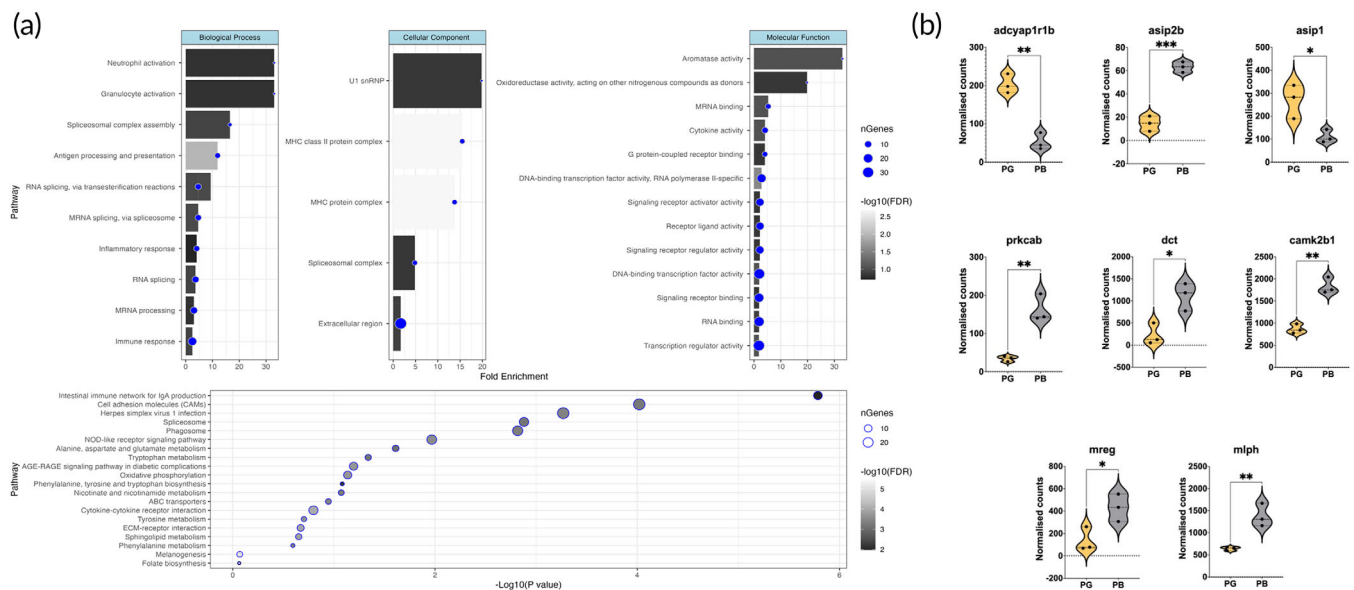


FIGURE 3 (a) Most significant GOs (from left to right) biological processes, cellular components, and molecular function. Bottom: most significant Kyoto Encyclopedia of Genes and Genomes (KEGGs). (b) Violin plots representing the expression of selected genes related to the melanin production pathway. The normalized counts are plotted across PG and PB. y axes: normalized counts; x axis, color variants (PG and PB). ***p < 0.001, **p < 0.01, *p < 0.05.

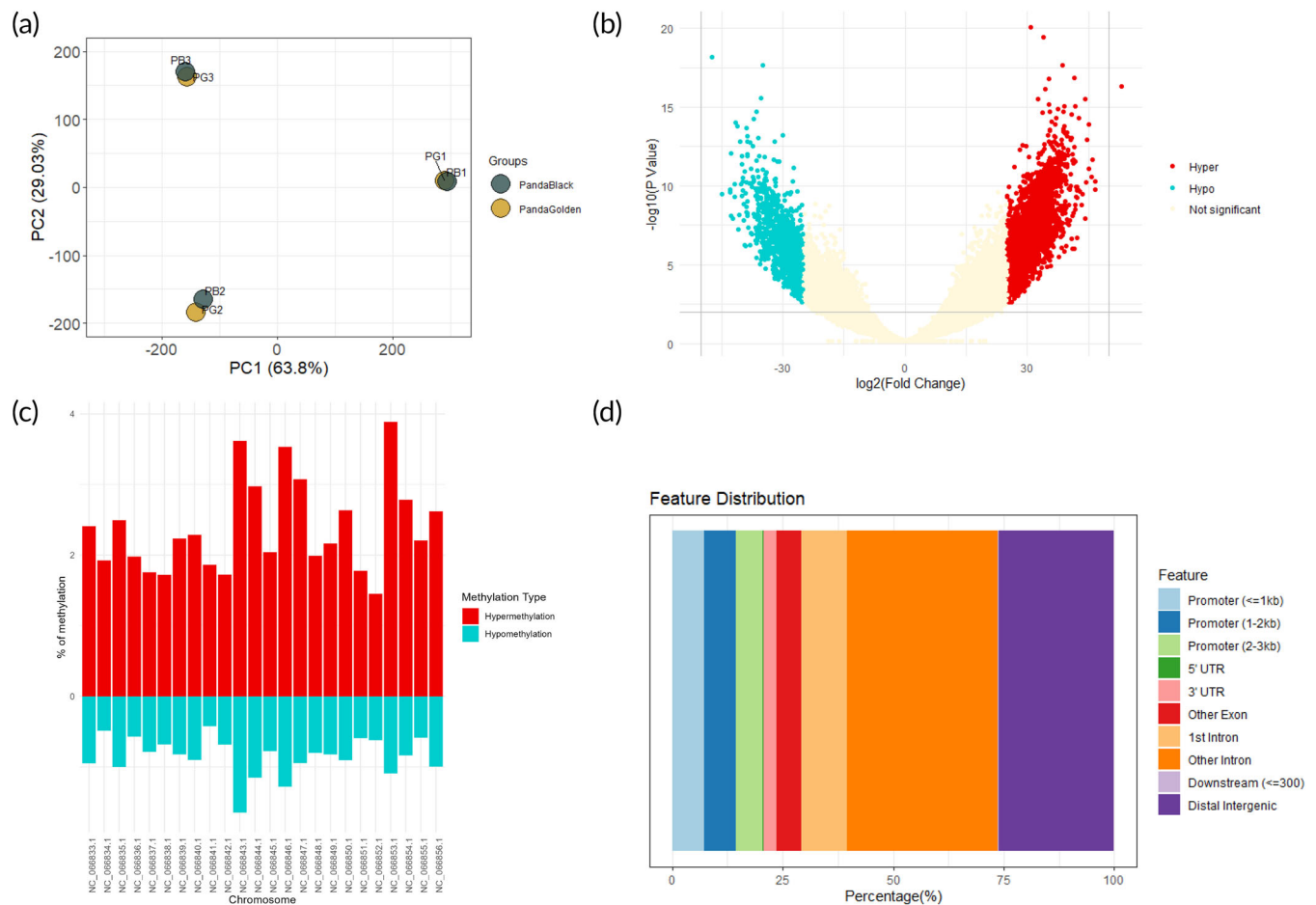


FIGURE 4 (a) Principal coordinates analysis (PCA) of methylation patterns of color variants (PG, “panda golden”; PB, “panda black”) of *Lates calcarifer*. (b) Volcano plot representing significant differentially methylated cytosine (DMC) between PG and PB barramundi. Blue, hypomethylated; red, hypermethylated. (c) Methylation percentage (%) per chromosome. Red, hypermethylation; blue, hypomethylation. (d) Genomic feature distribution of DMC.

29.03%) (Figure 4a). Samples from the same individual clustered tightly in multidimensional space, no matter the color differences (Data S5). The PCA correlation among skin colors, utilizing the total 160,460 CpG positions, were also analyzed; the PCA showed that 74.22% of the methylation profile was explained by the first three principal components (PC1 = 29.07%, PC2 = 24.81% and PC3 = 20.33%) (Data S6 and S7).

3.4.2 | Differentially methylated CpG

Comparing the methylation of CpGs in the fin between PG and PB, differential methylation analysis showed that 4877 DMCs ($>25\%$, $q < 0.01$) were significant. Of these, 1596 (26.57%) were hypomethylated and 3581 (73.43%) were hypermethylated (Figure 4b). The mean methylation per chromosome was homogeneous, with a higher percentage of hypermethylated DMCs than hypomethylated DMCs (Figure 4c).

Each DMC was mapped against the genome to determine the gene reference corresponding to the closest transcript site. A total of

4825 DMCs were mapped to a gene (in one of its multiple regions), yielding 3554 unique differentially methylated genes (DMGs). Genomic feature analysis revealed the different locations of the DMCs. Overall, 20.05% of the DMCs were located in the promoter region (<1 kb, 7.23%; 1–2 kb, 7.3%; 2–3 kb, 5.97%), 0.25% and 2.78% were located in the 5' untranslated region (UTR) and 3' UTR, respectively, 5.76% were located in exon regions, while 44.35% were located in introns (1st intron, 10.26%, other introns, 34.09%), and 0.169% of the DMCs were in the downstream (≤ 300) and 26.18% in the distal intergenic region (Figure 4d).

3.5 | Comparative analysis of DEGs and DMGs between PG and PB of the “panda” barramundi

To further analyze the data and identify putative functional DMCs, methylation analysis data were integrated with the previously analyzed transcriptome data (Section 4.1) where the RNA-sequencing (RNA-seq) analysis of PG and PB was analyzed. Among the two color variants, 1601 genes were found to have differential expression. The

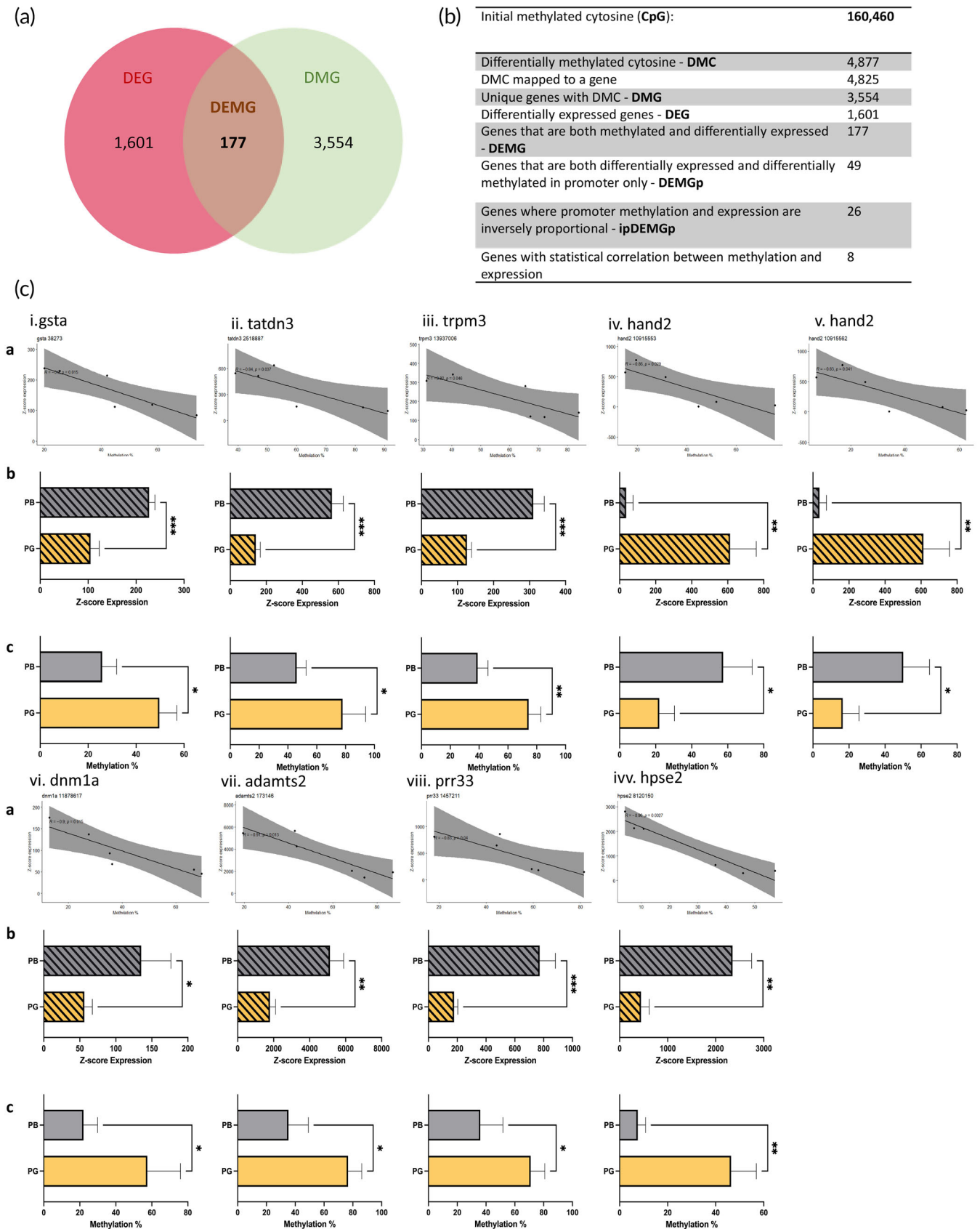


FIGURE 5 Legend on next page.

DEG list and Z-score for each gene were used to identify genes that were both differentially expressed and differentially methylated. Subsequently, 177 genes were identified as being concurrently differentially expressed and differentially methylated (differentially expressed-methylated genes [DEMGs]) (Figure 5a).

3.6 | Correlation between expression and methylation within DEMGs between PG and PB

Given that methylation variation at promoter regions has been shown to affect transcription activity and may thus play a role in phenotypic variation in the color of barramundi, we chose DEMGs with at least one DMC in the promoter region (DEMGp). We therefore selected 49 DEMGps, corresponding to 56 DMCs. To investigate the impact of the promoter DMC and expression of the corresponding gene, the relationship between methylation and expression was further investigated. The relationship between promoter methylation and expression is often reported as inversely proportional (Robertson & Jones, 2000). We therefore reported genes that were either hypermethylated-downregulated or hypomethylated-upregulated. A total of 30 DMCs were found with such a relationship, corresponding to 26 unique ipDEMGps (Data S8). Of these, nine DMCs had a significant negative correlation ($R < -0.5$, adj $p < 0.05$) between methylation and expression, corresponding to eight ipDEMGps (Data S9). The rational and results from the initial methylated cytosine to final statistically correlated genes are summarized in Figure 5a,b.

The relationship between the expression and methylation of the eight ipDEMGps is depicted in Figure 5c.x. The genes *gsta* (i), *tatdn3* (ii), *trpm3* (iii), *dnm1a* (vi), *adamts2* (vii), *pr33* (viii), and *hpse2* (ivv) exhibited a consistent pattern of expression and methylation. Specifically, PB expression was increased compared to PG (Figure 5c.y), and the promoter region was found to be hypermethylated in the PG (Figure 5c.z). The gene *hand2* (iv. and v.) exhibited an inverse pattern, with the promoter being identified as hypomethylated in PG (Figure 5c.z.iv,v) and the expression being downregulated in PB, as compared to PG (Figure 5c.y.iv,v).

4 | DISCUSSION

To investigate the molecular mechanisms behind the rare “panda” phenotype in *L. calcarifer*, this study integrated RNA-seq analysis and DNA methylation (WGEMS) data through a multiomics approach. The

study initially identified 1601 DEGs and 3554 DMGs between PG and PB patches of the “panda” barramundi. By combining the transcriptome and methylation data, 26 genes with a negative correlation between expression ratio and the percentage of methylation at the promoter region were identified. Among these, eight genes exhibited statistically significant associations. Additionally, several genes known to be associated with the pattern formation and pigmentation of teleosts were found to be differentially expressed.

4.1 | *asip* genes and their role in pattern formation

Prior research has emphasized the association between pigmentation and the presence, abundance, and interaction of chromatophores (Burton, 2011). In the case of barramundi, melanophores and xanthophores were found to be the primary pigment cells determining skin coloration (Marcoli et al., 2023): concentration and quantity of melanin and melanophores were described to be the main difference between the PG and PB patches of “panda” barramundi. Similar findings were found in zebrafish (*Danio rerio*), where the adult dark and light horizontal stripes are the result of the precise arrangement of pigment cells (Patterson & Parichy, 2019).

Several genes have been identified, particularly through studies involving mutations, as being implicated in the correct pattern formation in teleosts (Irion & Nüsslein-Volhard, 2019) and pigment transportation (Hu et al., 2021). The *agouti* gene (also known as the *asip* gene) has long been known as responsible for countershading pattern formation in vertebrates (Cal, 2017) and encodes for the Agouti-signaling protein. It has been demonstrated that in many teleosts the expression of this gene follows a dorso-ventral expression, with increases in expression from the dorsal to the ventral positioned skin, resulting in the countershading pattern (Irion & Nüsslein-Volhard, 2019). In fact, high *asip* gene expression is known to be associated with reduced melanogenesis as the agouti-signaling protein binds to the *mc1r* receptor, leading to light coloration in mammals (production of pheomelanin) and melanin production inhibition in teleosts (Cal et al., 2017). Significantly, a study on Oujiang colored common carp (*Cyprinus carpio* var. *color*) examined the expression of the *asip* gene in both the black and white patches of the same individual (Chen et al., 2019). The findings revealed that the expression of *asip* gene not only played a role in the ancestral dorso-ventral pattern formation of common carp, but also had a connection to the formation of black patches, specifically the black patches exhibited a statistically lower expression of the *asip* gene, compared to the white ones (Chen et al., 2019). Similar results were also found in pseudo-albino

FIGURE 5 (a) Venn diagram representing the number of differentially expressed genes (DEGs) in green, differentially methylated gene (DMG) in pink, and differentially expressed-methylated gene (DEMG) in brown. (b) Table summarizing the rational and results from initial methylated cytosine to final genes with statistical correlation between methylation at promoter and expression. (c) x. Correlation between methylation and expression of genes with statistical correlation in the “panda” phenotype of *Lates calcarifer*. y. Z-score expression of PB (“panda black”) and PG (“panda golden”). z. Methylation percentage of PB and PG. i. *Gsta* (LOC108893003), ii. *Tatdn3* (LOC108887491), iii. *Trpm3* (LOC 108878432) iv. *Hand2*-10,915,553 (LOC108872743), v. *Hand2*-10,915,562 (LOC108872743), vi. *Dnm1a* (LOC108874455), vii. *Adamts2* (LOC108873642), viii. *pr33* (LOC108902713), ivv. *Hpse2* (LOC108884124).

cultured turbot (*Scophthalmus maximus*), where the expression of the *asip1* gene was statistically upregulated in the non-pigmented patches, compared to the pigmented ones, in both dorsal and ventral skin (Guillot et al., 2012). In the present study involving “panda” barramundi, the expression of the *asip1* gene was found to be upregulated in the PG and downregulated in the PB, highlighting the possible role of this gene on the onset of the pattern formation. Additionally, a second copy of the *asip* gene (*asip2b*) was also found to be differentially expressed and having an opposite pattern of expression to the *asip1* gene (up regulated in PB and downregulated in PG) between the two-color patches of barramundi. The presence of multiple copies of the *asip* gene has been found within the genome of both mammals (Norris & Whan, 2008) and teleosts (Kang & Kim, 2023; Liang et al., 2021). The different role between *asip1* and *asip2b* (also known as *agrp2*) has been described previously (Liang et al., 2021), where *asip2b* is thought to be a “global stripe repressor”. To demonstrate this, the expression of this gene was found to be significantly higher in non-striated species (compared to the striped ones) of the subfamily *Danioninae* (Liang et al., 2021). Additionally, similarly to what was found in our present study between golden and black patches, the expression of *asip1* and *asip2b* was found to have opposite expression between yellow and black vertical stripes in *Haplochromis latifasciatus* (Liang et al., 2020). It has been suggested that *asip1* and *asip2b* have contrasting functions in pigment dispersion and chromatophore proliferation, where *asip1* acts as a repressor, while *asip2b* acts as a stimulator (fig. 1 from Cal et al., 2017). Hence, it is plausible that the combination of differential expression of the two *asip* genes in barramundi may play a role in determining pattern formation in this species.

4.2 | Genes related to melanosomal trafficking

Several genes involved in melanosomal trafficking were found to be differentially expressed between the PG and PB patches of barramundi. Melanosomes are organelles within the melanophore that contain melanin. The balance between anterograde and retrograde transport determines how these organelles aggregate or disperse within the melanophore, ultimately determining the lightening or darkening of the skin (Scott, 2006). Rab36 and melanoregulin are recognized to function as cargo receptors on melanosomes for retrograde transport (Maruta & Fukuda, 2022). Melanoregulin is the product of the *mreg* gene, and its alteration has been correlated to changes in pigmentation in mammals (Wu et al., 2012), as well as in teleosts (Henning et al., 2013; Ng'oma et al., 2014). Differences in melanoregulin expression were also found between golden and wildtype Midas cichlid (*Amphilophus citrinellu*), where *mreg* was found to be downregulated in the golden phenotype (Henning et al., 2013). Similarly, *mreg* was differentially expressed between the yellow tail morph and red tail morph from F2 progeny from *N. furzeri* × *N. kadleci* (Ng'oma et al., 2014). Consistent with these findings in other teleosts, the *mreg* gene was found downregulated in the PG barramundi variant compared to the PB, highlighting the possible role of this gene in barramundi pigmentation.

Another gene involved in melanosome transport is the *mlph* gene. This gene provides instruction for the protein melanophillin,

responsible, alongside with the proteins MyoVa and Rab27a, with the trafficking of melanosomes. While MyoVa and Rab27a play a broader role in vesicle trafficking (Fukuda, 2021; Langford, 2002), melanophillin is thought to be dedicated to the melanosome only (Kuroda et al., 2003). Loss of function and dysregulation of this gene have been associated with pigmentation changes (color dilution) in many vertebrates, including quail (Yuan et al., 2023), dog (Drögemüller et al., 2007), American mink (Cirera et al., 2013), goat (Li et al., 2010), python (Lederer et al., 2023), zebrafish (Sheets et al., 2007), and Oujiang color common carp (Philipp et al., 2005). In barramundi, the expression of the *mlph* gene was found to be downregulated in PG, in comparison to the PB patches. Similar results were found in a study undertaken on the Oujiang color common carp, where two phenotypes with double color patches, WB (white and black patches) and RB (red and black patches), were analyzed. In both phenotypes, the black patches exhibited a significantly higher expression of *mlph1* compared to the red/white spots (Hu et al., 2021).

Additionally, in zebrafish, a novel function of melanophillin has been proposed; melanophillin is proposed to independently regulate dynein, a protein responsible for melanosome trafficking (Sheets et al., 2007). Interestingly, in barramundi, dynamin gene (*dnm1a*) was one of the eight ipDEMg genes, where its expression was upregulated in PB, in comparison to the PG, and the promoter was hypermethylated in the PG. Dynamin is a putative protein identified in melanosomes, alongside dynein, dynactin, kinesin, and myosin Va (Aktary et al., 2021), and plays a pivotal role in vesicle trafficking (Vaman et al., 2015), as well as having an important binding function with melanophillin/slac2-a (Aktary et al., 2021). It is therefore possible that the differential methylation (and consequential differential expression) of dynamin could have an important role in the “panda” pattern formation in barramundi.

Other genes that have been found to be involved in melanosome trafficking are *adcyap1rs*, coding for the pituitary adenylate cyclase-activating polypeptide (PACAP) receptors. Although the PACAP and its receptors are widely expressed and play a variety of roles in vertebrate physiology, it is also known that variations in their expression are linked to the regulation of skin pigmentation in frogs (Tang et al., 2014) and teleosts such as catfish (*Clarias gariepinus*) (Lugo et al., 2008). In our present study, *adcyap1r1b*, one of the PACAP receptors, was found to be upregulated in PG barramundi in comparison to PB. Similar results were found in speckled tilapia (*Oreochromis mossambicus*), where the dark and light color skin were analyzed, and the expression of *adcyap1r1a* was found to be upregulated in the lighter skin (Cardoso et al., 2015); within the same study the expression of *adcyap1r1b* was found to be not altered between the two color forms, thus it is possible that the expression of these genes is species specific.

4.3 | *hand2* and its role in “panda” barramundi coloration

The *hand2* gene was found within the eight genes with a statistical correlation between expression and methylation. This gene encodes

for the heart- and neural crest derivatives-expressed protein 2 protein, a multifunctional DNA binding protein affecting differentiation and cell type specific gene expression in the neural crest (Hendershot et al., 2008). Alteration of the expression of this gene results in a significant loss of neurons, as well as significant reduction of *TH* expression (Hendershot et al., 2008). *TH* encodes for the enzyme tyrosine hydroxylase, which is essential for the normal functioning of the nervous system, but has also a role in the melanin synthesis, by converting L-tyrosinase to L-dihydroxyphenylalanine (Ferreira et al., 2023). Additionally, *Hand2* is known to positively affect the regulation of *alx3* (Funato et al., 2016), whose main role is correlated to skeletal development (Beverdam et al., 2001). Remarkably, a recent study undertaken on chipmunks showcased the evident role of *alx3* in the stripe pattern formation in rodents (Mallarino et al., 2016), where *alx3* acts as a transcription factor repressing *mitf*, therefore promoting light colored pheomelanin biosynthesis (Mallarino et al., 2016). In “panda” barramundi, *alx3* was found to be downregulated in PG. This result could be explained by the basic difference in pigmentation production between mammals and teleosts, where, in fish, the difference in coloration is not due to biochemical changes in the biosynthesis of pheomelanin/eumelanin, but rather to the presence/absence of certain cells (Kottler et al., 2015). *hand2* methylation and differential expression could therefore be a core molecular driver in the mechanism characterizing the two colorations of “panda”, as a direct regulator of *alx3*.

5 | CONCLUSION

Our study highlights the differential expression of genes involved in melanosome trafficking and chromatophore differentiation. Several genes, exhibiting both differential expression and methylation, may influence the onset of the “panda” pattern in barramundi and although the coloration difference between PG and PB could not be attributed to a single gene, a list of candidate genes were identified. Methylation appears to be implicated in the phenotypic variation, suggesting that the trait is under epigenetic regulation. For future exploration, it would be of interest utilizing CRISPR-Cas9 trials targeting the genes found within this research, as a proof of concept.

Additionally, following the precedent studies on koi carp (Luo et al., 2018), microRNA may play a significant role in barramundi color differentiation, alongside DNA methylation. Further investigation into microRNA could provide deeper insights into the underlying molecular mechanisms shaping the distinct color patches. Because of the plasticity of the “panda” pattern phenotype, a comprehensive study with multiple sampling times during pattern changes may further unravel these intricate mechanisms.

To conclude, our study identifies crucial genes with both differential expression and methylation, providing crucial information and the basis for future investigations into barramundi pattern formation. Additionally, barramundi could serve as a valuable model for studying skin pattern formation and modification in teleosts, providing insights into the blotch-like pattern formation.

AUTHOR CONTRIBUTIONS

Conceptualisation: MR, JDR. Methodology: MR. Validation, formal analysis, investigation: MR. Resources: JDR, HPJ and CHS. Writing – Original Draft: MR. Writing – Review and Editing: JDR, JDB, HPJ. Visualisation: MR. Supervision: MR, JDR. Funding acquisition: JDR, JDB, HPJ and CHS.

ACKNOWLEDGMENTS

We would like to acknowledge our funding body, the Australian Research Council, through the found scheme Linkage, with the grant title: “Striking Gold: Determining the genetic drivers of gold coloration in barramundi”, ID: LP200201003. We would also like to acknowledge Dr. Jarrod Guppy for his support and help during the sampling collection. Open access publishing facilitated by James Cook University, as part of the Wiley - James Cook University agreement via the Council of Australian University Librarians.

CONFLICT OF INTEREST STATEMENT

The authors declare the following financial interests/personal relationships which may be considered as potential competing interests: Roberta Marcoli reports financial support was provided by the Australian Research Council.

ORCID

Roberta Marcoli  <https://orcid.org/0000-0002-3483-6899>

REFERENCES

- Ahi, E. P., & Sefc, K. M. (2017). A gene expression study of dorso-ventrally restricted pigment pattern in adult fins of neolamprologus meeli, an african cichlid species. *PeerJ*, 5, e2843.
- Akalin, A., Kormaksson, M., Li, S., Garrett-Bakelman, F. E., Figueroa, M. E., Melnick, A., & Mason, C. E. (2012). MethylKit: A comprehensive R package for the analysis of genome-wide DNA methylation profiles. *Genome Biology*, 13, R87.
- Aktary, Z., Conde-Perez, A., Rambow, F., Di Marco, M., Amblard, F., Hurbain, I., Raposo, G., Delevoye, C., Coscoy, S., & Larue, L. (2021). A role for *dynl1c3* in melanosome movement, distribution, acidity and transfer. *Communications Biology*, 4(1), 423.
- Andrews, S. (2010). *Fastqc: A quality control tool for high throughput sequence data*. In. *Fastqc: A quality control tool for high throughput sequence data: Babraham bioinformatics*. Babraham Institute.
- Beverdam A, Brouwer A, Reijnen M, Korving J, Meijlink F. (2001). Severe nasal clefting and abnormal embryonic apoptosis in *Alx3/Alx4* double mutant mice. *Development*. 128(20), 3975–3986. <https://doi.org/10.1242/dev.128.20.3975>
- Burton D. *The skin| coloration and chromatophores in fishes*. 2011. Elsevier.
- Cal L. *Fish pigmentation: Functional and evolutionary characterization of the agouti locus*. 2017. (Doctoral dissertation, Universidade de Vigo).
- Cal, L., Suarez-Bregua, P., Cerdá-Reverter, J. M., Braasch, I., & Rotllant, J. (2017). Fish pigmentation and the melanocortin system. *Comparative Biochemistry and Physiology Part A: Molecular & Integrative Physiology*, 211, 26–33.
- Cal, L., Suarez-Bregua, P., Comesaña, P., Owen, J., Braasch, I., Kelsh, R., Cerdá-Reverter, J. M., & Rotllant, J. (2019). Countershading in zebrafish results from an *asip1* controlled dorsoventral gradient of pigment cell differentiation. *Scientific Reports*, 9(1), 3449.
- Cardoso, J. C., Felix, R. C., Martins, R. S., Trindade, M., Fonseca, V. G., Fuentes, J., & Power, D. M. (2015). Pacap system evolution and its role

- in melanophore function in teleost fish skin. *Molecular and Cellular Endocrinology*, 411, 130–145.
- Chen, H., Wang, J., Du, J., Si, Z., Yang, H., Xu, X., & Wang, C. (2019). Asip disruption via crispr/cas9 system induces black patches dispersion in oujiang color common carp. *Aquaculture*, 498, 230–235.
- Cirera, S., Markakis, M. N., Christensen, K., & Anistoroaei, R. (2013). New insights into the melanophilin (mlph) gene controlling coat color phenotypes in American mink. *Gene*, 527(1), 48–54.
- Dong, Z., Luo, M., Wang, L., Yin, H., Zhu, W., & Fu, J. (2020). MicroRNA-206 regulation of skin pigmentation in koi carp (*Cyprinus carpio* L.). *Frontiers in Genetics*, 11, 47.
- Drögemüller, C., Philipp, U., Haase, B., Günzel-Apel, A.-R., & Leeb, T. (2007). A noncoding melanophilin gene (mlph) snp at the splice donor of exon 1 represents a candidate causal mutation for coat color dilution in dogs. *Journal of Heredity*, 98(5), 468–473.
- Ewels, P., Magnusson, M., Lundin, S., & Käller, M. (2016). Multiqc: Summarize analysis results for multiple tools and samples in a single report. *Bioinformatics*, 32(19), 3047–3048.
- Fang, W., Huang, J., Li, S., & Lu, J. (2022). Identification of pigment genes (melanin, carotenoid and pteridine) associated with skin color variant in red tilapia using transcriptome analysis. *Aquaculture*, 547, 737429.
- Ferreira, A. M., de Souza, A. A., Koga, R. C. R., Sena, I. S., Matos, M. J. S., Tomazi, R., Ferreira, I. M., & Carvalho, J. C. T. (2023). Anti-melanogenic potential of natural and synthetic substances: Application in zebrafish model. *Molecules*, 28(3), 1053.
- Fukuda, M. (2021). Rab gtpases: Key players in melanosome biogenesis, transport, and transfer. *Pigment Cell & Melanoma Research*, 34(2), 222–235.
- Funato, N., Kokubo, H., Nakamura, M., Yanagisawa, H., & Saga, Y. (2016). Specification of jaw identity by the hand2 transcription factor. *Scientific Reports*, 6(1), 28405.
- Guillot, R., Ceinos, R. M., Cal, R., Rotllant, J., & Cerda-Reverter, J. M. (2012). Transient ectopic overexpression of agouti-signalling protein 1 (asip1) induces pigment anomalies in flatfish. *PLoS One*, 7(12), e48526.
- Gur, D., Bain, E. J., Johnson, K. R., Aman, A. J., Pasolli, H. A., Flynn, J. D., Allen, M. C., Deheyn, D. D., Lee, J. C., & Lippincott-Schwartz, J. (2020). In situ differentiation of iridophore crystalloids underlies zebrafish stripe patterning. *Nature Communications*, 11(1), 6391.
- Hendershot, T. J., Liu, H., Clouthier, D. E., Shepherd, I. T., Coppola, E., Studer, M., Firulli, A. B., Pittman, D. L., & Howard, M. J. (2008). Conditional deletion of hand2 reveals critical functions in neurogenesis and cell type-specific gene expression for development of neural crest-derived noradrenergic sympathetic ganglion neurons. *Developmental Biology*, 319(2), 179–191.
- Henning, F., Jones, J. C., Franchini, P., & Meyer, A. (2013). Transcriptomics of morphological color change in polychromatic midas cichlids. *BMC Genomics*, 14(1), 1–14.
- Hu, X., Chen, H., Yu, L., Chen, X., Mandal, B. K., Wang, J., & Wang, C. (2021). Functional differentiation analysis of duplicated mlpha gene in oujiang color common carp (*Cyprinus carpio* var. *color*) on colour formation. *Aquaculture Research*, 52(10), 4565–4573.
- Irion, U., & Nüsslein-Volhard, C. (2019). The identification of genes involved in the evolution of color patterns in fish. *Current Opinion in Genetics & Development*, 57, 31–38.
- Jerry, D. R. (2013). *Biology and culture of Asian seabass Lates calcarifer*. CRC Press.
- Johnson, S. L., Africa, D., Walker, C., & Weston, J. A. (1995). Genetic control of adult pigment stripe development in zebrafish. *Developmental Biology*, 167(1), 27–33.
- Kang, D.-Y., & Kim, H.-C. (2023). Functional relation of agouti signaling proteins (ASIPs) to pigmentation and color change in the starry flounder, *Platichthys stellatus*. *Comparative Biochemistry and Physiology Part A: Molecular & Integrative Physiology*, 189, 111524.
- Kondo, S., Watanabe, M., & Miyazawa, S. (2021). Studies of turing pattern formation in zebrafish skin. *Philosophical Transactions of the Royal Society A*, 379(2213), 20200274.
- Kottler, V. A., Künstner, A., & Scharlt, M. (2015). Pheomelanin in fish? *Pigment Cell & Melanoma Research*, 28(3), 355–356.
- Kratochwil, C. F., & Mallarino, R. (2023). Mechanisms underlying the formation and evolution of vertebrate color patterns. *Annual Review of Genetics*, 57, 135–156.
- Krueger, F., James, F., Ewels, P., Afyounian, E., & Schuster-Boeckler, B. (2021). Felixkrueger/trimgalore: V0. 6.7-doi via zenodo. <https://zenodo.org/record/5127899> (accessed February 23, 2022).
- Kuroda, T. S., Ariga, H., & Fukuda, M. (2003). The Actin-binding domain of slac2-a/melanophilin is required for melanosome distribution in melanocytes. *Molecular and Cellular Biology*, 23(15), 5245–5255.
- Langford, G. M. (2002). Myosin-v, a versatile motor for short-range vesicle transport. *Traffic*, 3(12), 859–865.
- Lederer, I., Shahid, B., Dao, U., Brogdon, A., Byrtus, H., Delva, M., Deva, O., Hatfield, P., Hertz, M., & Justice, J. (2023). A frameshift variant in the melanophilin gene is associated with loss of pigment from shed skin in ball pythons (*python regius*). *Micropublication Biology*, 2023, <https://doi.org/10.17912/micropub.biology.000896>
- Li, H., Handsaker, B., Wysoker, A., Fennell, T., Ruan, J., Homer, N., Marth, G., Abecasis, G., Durbin, R., & Subgroup, G. P. D. P. (2009). The sequence alignment/map format and samtools. *Bioinformatics*, 25(16), 2078–2079.
- Li, X.-L., Feng, F.-J., Zhou, R.-Y., Li, L.-H., Zheng, H., & Zheng, G. (2010). Nine linked snps found in goat melanophilin (mlph) gene. *Journal of Bioinformatics and Sequence Analysis*, 2(6), 85–90.
- Li, X.-M., Song, Y.-N., Xiao, G.-B., Zhu, B.-H., Xu, G.-C., Sun, M.-Y., Xiao, J., Mahboob, S., Al-Ghanim, K. A., & Sun, X.-W. (2015). Gene expression variations of red–White skin coloration in common carp (*Cyprinus carpio*). *International Journal of Molecular Sciences*, 16(9), 21310–21329.
- Liang, Y., Gerwin, J., Meyer, A., & Kratochwil, C. F. (2020). Developmental and cellular basis of vertical bar color patterns in the East African cichlid fish *Haplochromis latifasciatus*. *Frontiers in Cell and Developmental Biology*, 8, 62.
- Liang, Y., Grauvogl, M., Meyer, A., & Kratochwil, C. F. (2021). Functional conservation and divergence of color-pattern-related agouti family genes in teleost fishes. *Journal of Experimental Zoology Part B: Molecular and Developmental Evolution*, 336(5), 443–450.
- Liu, L., Wang, X., Zhang, R., Li, H., & Zhu, H. (2022). Cell junction and vesicle trafficking-mediated melanosome/melanin transfer are involved in the dynamic transformation of goldfish *Carassius auratus* skin color. *International Journal of Molecular Sciences*, 23(20), 12214.
- Love, M. I., Huber, W., & Anders, S. (2014). Moderated estimation of fold change and dispersion for RNA-seq data with deseq2. *Genome Biology*, 15(12), 1–21.
- Lugo, J. M., Rodriguez, A., Helguera, Y., Morales, R., Gonzalez, O., Acosta, J., Besada, V., Sanchez, A., & Estrada, M. P. (2008). Recombinant novel pituitary adenylate cyclase-activating polypeptide from african catfish (*Clarias gariepinus*) authenticates its biological function as a growth-promoting factor in low vertebrates. *Journal of Endocrinology*, 197(3), 583.
- Luo, M., Wang, L., Zhu, W., Fu, J., Song, F., Fang, M., Dong, J., & Dong, Z. (2018). Identification and characterization of skin color micromRNAs in koi carp (*Cyprinus carpio* L.) by illumina sequencing. *BMC Genomics*, 19, 1–15.
- Mallarino, R., Henegar, C., Mirasierra, M., Manceau, M., Shradin, C., Vallejo, M., Beronja, S., Barsh, G. S., & Hoekstra, H. E. (2016). Alx3 regulates the spatial differences in hair pigment underlying stripe patterns in rodents. *Nature*, 539(7630), 518–523.
- Marcoli, R., Jones, D. B., Massault, C., Marc, A. F., Moran, M., Harrison, P. J., Cate, H. S., Lopata, A. L., & Jerry, D. R. (2023). The skin structure in multiple color variants of barramundi (*Lates calcarifer*): A

- histological, immunohistochemical and ultrastructural overview. *Aquaculture*, 576, 739859.
- Marcoli, R., Jones, D. B., Massault, C., Moran, M., Harrison, P. J., Cate, H. S., & Jerry, D. R. (2024). Revealing the genetic and molecular drivers behind golden and platinum coloration in barramundi (*Lates calcarifer*). *Aquaculture*, 586, 740820.
- Maruta, Y., & Fukuda, M. (2022). Large rab gtpase rab44 regulates microtubule-dependent retrograde melanosome transport in melanocytes. *Journal of Biological Chemistry*, 298(11), 102508.
- Mhanni, A. A., & McGowan, R. A. (2002). Variations in DNA (cytosine-5)-methyltransferase-1 expression during oogenesis and early development of the zebrafish. *Development Genes and Evolution*, 212(11), 530–533.
- Moore, L. D., Le, T., & Fan, G. (2013). DNA methylation and its basic function. *Neuropsychopharmacology*, 38(1), 23–38.
- Ng'oma, E., Groth, M., Ripa, R., Platzer, M., & Cellerino, A. (2014). Transcriptome profiling of natural dichromatism in the annual fishes *Nothobranchius furzeri* and *Nothobranchius kadleci*. *BMC Genomics*, 15(1), 754.
- Norris, B. J., & Whan, V. A. (2008). A gene duplication affecting expression of the ovine asip gene is responsible for white and black sheep. *Genome Research*, 18(8), 1282–1293.
- Patterson, L. B., & Parichy, D. M. (2019). Zebrafish pigment pattern formation: Insights into the development and evolution of adult form. *Annual Review of Genetics*, 53, 505–530.
- Pedersen, B. S., Eyring, K., De, S., Yang, I. V., & Schwartz, D. A. (2014). Fast and accurate alignment of long bisulfite-seq reads. arXiv Preprint arXiv:1401.1129.
- Philipp, U., Quignon, P., Scott, A., Andre, C., Breen, M., & Leeb, T. (2005). Chromosomal assignment of the canine melanophilin gene (mlph): A candidate gene for coat color dilution in pinschers. *Journal of Heredity*, 96(7), 774–776.
- Robertson, K. D. A., & Jones, P. (2000). DNA methylation: Past, present and future directions. *Carcinogenesis*, 21(3), 461–467.
- Santos, M. E., Baldo, L., Gu, L., Boileau, N., Musilova, Z., & Salzburger, W. (2016). Comparative transcriptomics of anal fin pigmentation patterns in cichlid fishes. *BMC Genomics*, 17(1), 712.
- Scott, G. A. (2006). Melanosome trafficking and transfer. *The Pigmentary System: Physiology and Pathophysiology*, 494, 171–180.
- Sheets, L., Ransom, D. G., Mellgren, E. M., Johnson, S. L., & Schnapp, B. J. (2007). Zebrafish melanophilin facilitates melanosome dispersion by regulating dynein. *Current Biology*, 17(20), 1721–1734.
- Singh, A. P., & Nüsslein-Volhard, C. (2015). Zebrafish stripes as a model for vertebrate colour pattern formation. *Current Biology*, 25(2), R81–R92.
- Tang, Z.-J., Lue, S.-I., Tsai, M.-J., Yu, T.-L., Thiyagarajan, V., Lee, C.-H., Huang, W.-T., & Weng, C.-F. (2014). The hormonal regulation of color changes in the sexually dichromatic frog *Buergeria robusta*. *Physiological and Biochemical Zoology*, 87(3), 397–410.
- Tian, X., Peng, N.-n., Ma, X., Wu, L.-m., Shi, X., Liu, H.-f., Song, H.-m., Wu, Q.-s., Meng, X.-l., & Li, X.-j. (2022). MicroRNA-430b targets scavenger receptor class b member 1 (scarb1) and inhibits coloration and carotenoid synthesis in koi carp (*Cyprinus carpio* L.). *Aquaculture*, 546, 737334.
- Vaman, V. S. A., Poppe, H., Houben, R., Grunewald, T. G., Goebeler, M., & Butt, E. (2015). Lasp1, a newly identified melanocytic protein with a possible role in melanin release, but not in melanoma progression. *PLoS One*, 10(6), e0129219.
- Vij, S., Kuhl, H., Kuznetsova, I. S., Komissarov, A., Yurchenko, A. A., Van Heusden, P., Singh, S., Thevasagayam, N. M., Prakki, S. R. S., & Purushothaman, K. (2016). Chromosomal-level assembly of the Asian seabass genome using long sequence reads and multi-layered scaffolding. *PLoS Genetics*, 12(4), e1005954.
- Wu, X. S., Masedunskas, A., Weigert, R., Copeland, N. G., Jenkins, N. A., & Hammer, J. A. (2012). Melanoregulin regulates a shedding mechanism that drives melanosome transfer from melanocytes to keratinocytes. *Proceedings of the National Academy of Sciences*, 109(31), E2101–E2109.
- Yamaguchi, M., Yoshimoto, E., & Kondo, S. (2007). Pattern regulation in the stripe of zebrafish suggests an underlying dynamic and autonomous mechanism. *Proceedings of the National Academy of Sciences*, 104(12), 4790–4793.
- Yuan, Z., Zhang, X., Pang, Y., Qi, Y., Wang, Q., Hu, Y., Zhao, Y., Ren, S., & Huo, L. (2023). Association analysis of melanophilin (mlph) gene expression and polymorphism with plumage color in quail. *Archives Animal Breeding*, 66(1), 131–139.
- Zerulla, T. C., & Stoddard, P. K. (2021). The biology of polymorphic melanic side-spotting patterns in poeciliid fishes. *Frontiers in Ecology and Evolution*, 8, 608289.
- Zhang, Y. Q., Liu, J. H., Peng, L. Y., Ren, L., Zhang, H. Q., Zou, L. J., Liu, W. B., & Xiao, Y. M. (2017). Comparative transcriptome analysis of molecular mechanism underlying gray-to-red body color formation in red crucian carp (*Carassius auratus*, red var.). *Fish Physiology and Biochemistry*, 43(5), 1387–1398.

SUPPORTING INFORMATION

Additional supporting information can be found online in the Supporting Information section at the end of this article.

How to cite this article: Marcoli, R., Jones, D. B., Massault, C., Harrison, P. J., Cate, H. S., & Jerry, D. R. (2024). Barramundi (*Lates calcarifer*) rare coloration patterns: a multiomics approach to understand the “panda” phenotype. *Journal of Fish Biology*, 105(4), 1268–1279. <https://doi.org/10.1111/jfb.15892>